Supplementary Information for

Fabrication of tetraethyl orthosilicate / ethanol - water surfactant-free microemulsions and their applications in self-templating synthesis of monodispersed silica colloidal spheres

Jiahan Lu, Longhua Peng, Ao zhang, Jiaqiong Xu, Min Wu, and Shiyu Ma *

Research Center for Water Resources and Interface Science, School of Chemistry and Molecular Engineering, East China Normal University, Shanghai 200062, PR China

* Corresponding authors.

E-mail address: syma@chem.ecnu.edu.cn (S.Y. Ma).

1 Experimental section

1.1 Materials and reagents

TEOS was purchased from Sinopharm Group Chemical Reagents Co., Ltd (Shanghai, China). Ammonium hydroxide (28-30 wt%) was purchased from Shanghai Aladdin Biochemical Technology Co., Ltd (Shanghai, China). n-Propanol (NPA) and isopropanol (IPA) were purchased from Shanghai Marel Biochemical Technology Co. Ltd (Shanghai, China). TEOS, NPA and IPA were analytical grade chemicals and ammonium hydroxide was ACS grade chemicals. All chemicals were used without further purification. Ultrapure water with a resistivity of 18.25 MΩ cm was used throughout the experiments.

1.2 Apparatus and measurements

An electrical conductivity meter (DDSJ-308F, Shanghai INESA Scientific Instruments Co., Ltd) with a DDSJ-0.1 electrode of cell constant 0.111 cm^{-1} was used to measure the conductivity of the TEOS/NPA-H_2O and TEOS/IPA-H_2O ternary system.TEM was carried out on a H-7000 electron microscope (Hitachi, Japan). The steps for phase diagram construction, electrical conductivity measurements and synthesis of silica products were consistent with the manuscript.

2 Supporting Analysis

2.1 Phase diagram of TEOS/NPA-H_2O and TEOS/IPA-H_2O ternary systems.

The phase diagram of the TEOS/NPA-H_2O and TEOS/IPA-H_2O system and microregions of the phase diagram were constructed by visual titration and electrical conductivity measurements, respectively. The results are shown in Fig. S2.

Based on the previous analyses, the single-phase region of the phase diagram of the TEOS/NPA-H_2O and TEOS/IPA-H_2O system to be distinctly classified into three microregions: I (O/W type SFMEs), III (BC type SFMEs) and II (W/O type SFMEs).

2.2 Effect of TEOS contents on the properties of silica products synthesized with the TEOS/IPA-H_2O and TEOS/NPA-H_2O ternary systems.

$System_{A1}$-$System_{A3}$, which contain a constant IPA-water mass ratio ($R_{W/I}$ = 0.43), NPA-water mass ratio ($R_{W/N}$ = 0.43) and different TEOS mass fractions, were selected as model systems for the synthesis of silica products. The TEM images of silica products are shown in Fig. S3.

It can be seen from Fig. S3, the MSCSs can only be synthesized in O/W type SFMEs. However, as the TEOS fraction further increased to *f*o = 0.17 ($System_{A2}$) and *f*o = 0.26 ($System_{A3}$), discrete silica spheres cannot be synthesized (Figs. S3b, S3c, S3e and S3f), they displayed strong aggregation behavior. This is similar to the phenomenon obtained when ethanol is used as a solvent. Therefore, there is a clear correlation between silica morphologies and mesostructures of SFMEs.

However, when *f*o = 0.26, for EtOH, BC type SFMEs are formed, whereas for IPA and NPA, W/O type SFMEs are formed. In addition, by comparing Fig. 1 and Fig. S2, we can see that the O/W type SFMEs of the ternary system are larger when EtOH is used as a solvent than when IPA and NPA are used as solvents and the multiple-phase region of the ternary system are larger when EtOH and NPA are used as solvents than when IPA are used as solvents. Therefore, different solvents affect the threshold for the formation of different mesotructures.

3 Supporting Figures and Tables

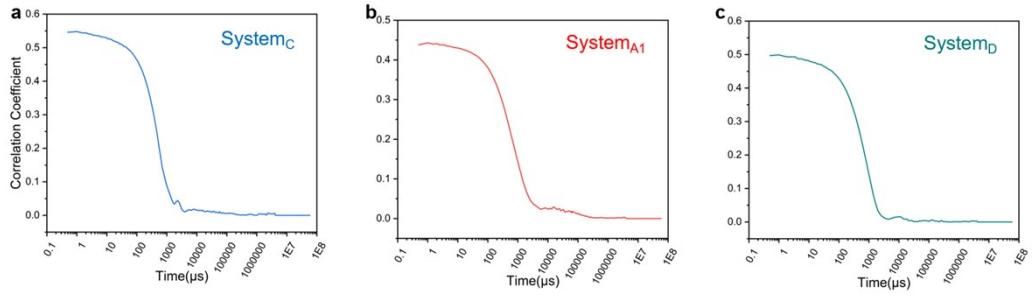

Fig. S1. Correlation coefficient function curves obtained by DLS measurements at 25±0.2 ℃.

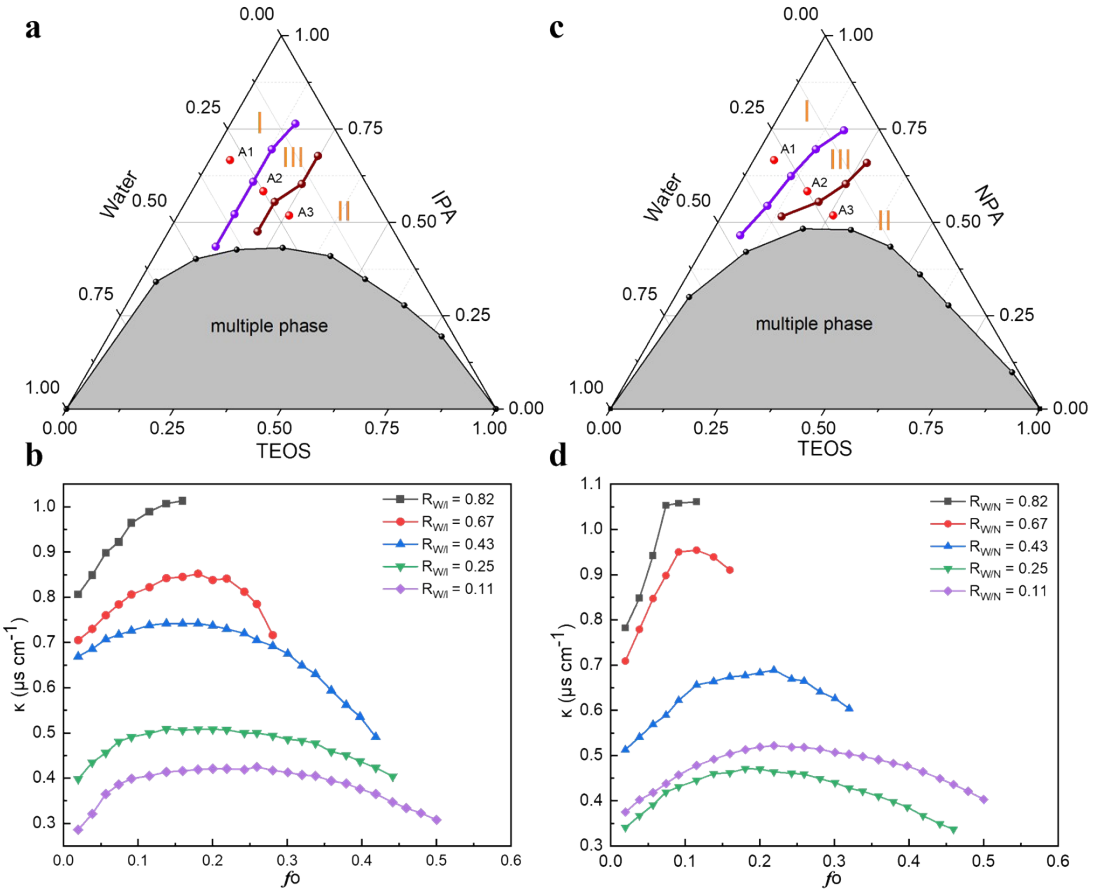

Fig. S2. (a) Phase diagram of the TEOS/IPA-H_2O ternary systems at 25 ± 0.2°C. I, III and II are O/W, BC and W/O microregions respectively. The points A1-A3, ($System_{A1}$-$System_{A3}$) were chosen for the synthesis of silica products, respectively. The content of each component is expressed by mass fraction. (b) Electrical conductivity κ as a function of *fo* at different $R_{W/I}$ values. (c) Phase diagram of the TEOS/NPA-H_2O ternary systems at 25 ± 0.2°C. I, III and II are O/W, BC and W/O microregions respectively. The points A1-A3, ($System_{A1}$-$System_{A3}$) were chosen for the synthesis of silica products, respectively. (d) Electrical conductivity κ as a function of *fo* at different $R_{W/N}$ values.

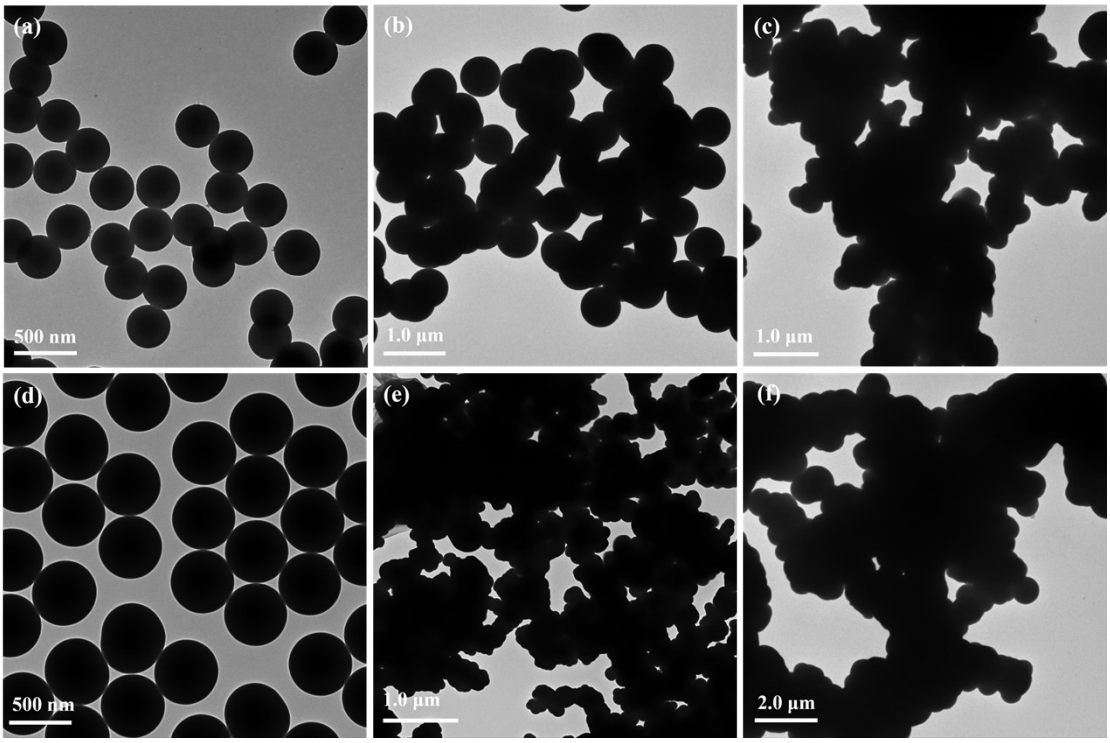

Fig. S3. (a-c) TEM images of the silica products synthesized with the TEOS/IPA-H_2O ternary systems with a constant $R_{W/I}$ = 0.43, same ammonia concentration and different TEOS mass fraction. (d-f) TEM images of the silica products synthesized with the TEOS/NPA-H_2O ternary systems with a constant $R_{W/N}$ = 0.43, same ammonia concentration and different TEOS mass fraction.

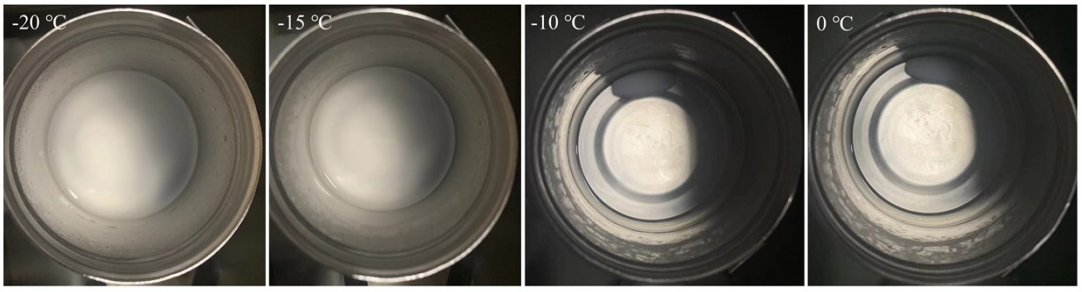

Fig. S4. Photographs of the $System_B$ at different cooling temperatures (-20 °C, -15 °C, -10 °C and 0 °C). The $System_B$ appears turbid at -20 °C and -15 °C.

Table S1. The yield of silica spheres synthesized with the $System_B$ at the cooling temperatures.

Strategy	-20 ℃	-15 ℃	-10 ℃	0 ℃
1	/	92.4 %	86.5 %	92.1 %
2	86.7 %	92.0 %	94.2 %	93.2 %

***** Strategy 1: the pre-reaction / low-temperature strategy. Strategy 2: the low-temperature equilibrium / reaction strategy.

Table S2. The chemical shift and condensation degree ($Q^2+Q^3/Q^2+Q^3+Q^4$) of those Q^n units of silica particles synthesized with the $System_B$ by the pre-reaction / low-temperature strategy.

Temperature	Chemical Shift of Q^2 (ppm)	Chemical Shift of Q^3 (ppm)	Chemical Shift of Q^4 (ppm)	$Q^2+Q^3/Q^2+Q^3+Q^4$
-15 ℃	-96.48 ± 0.10	-106.29 ± 0.02	-115.82 ± 0.02	44.79 %
-10 ℃	-97.06 ± 0.04	-105.93 ± 0.03	-115.48 ± 0.03	41.88 %
0 ℃	-92.90 ± 0.26	-102.81 ± 0.04	-112.03 ± 0.02	37.72 %